Journal of Power Sources 196 (2011) 808–813

Contents lists available at ScienceDirect

Journal of Power Sources

journal homepage: www.elsevier.com/locate/jpowsour

Reversible air electrodes integrated with an anion-exchange membrane for secondary air batteries

Naoko Fujiwara, Masaru Yao, Zyun Siroma, Hiroshi Senoh, Tsutomu Ioroi, Kazuaki Yasuda*

Research Institute for Ubiquitous Energy Devices, National Institute of Advanced Industrial Science and Technology (AIST), 1-8-31 Midorigaoka, Ikeda, Osaka 563-8577, Japan

ARTICLE INFO

Article history:
Received 1 July 2010
Received in revised form 22 July 2010
Accepted 26 July 2010
Available online 30 July 2010

Keywords:
Air electrode
Anion-exchange membrane
Oxygen reduction reaction
Oxygen evolution reaction
Metal–air battery
Carbon dioxide

ABSTRACT

Reversible air electrodes integrated with a polymer electrolyte membrane have been proposed for use in rechargeable metal–air batteries or unitized regenerative fuel cells to reduce the impact of atmospheric carbon dioxide. Reversible air electrodes were prepared with an anion-exchange membrane (AEM) as a polymer electrolyte membrane and platinum-based catalysts. The AEM at the interface between the alkaline electrolyte and the air electrode layer plays major roles in AEM-type air electrodes as follows: it blocks (a) the permeation of cations in the alkaline electrolyte into the air electrode layer to prevent carbonate precipitation, (b) penetration of the alkaline solution itself, and (c) neutralization of the alkaline electrolyte by carbon dioxide, all of which prevent performance degradation of oxygen reactions. Catalysts for decreasing the overvoltage of oxygen reactions were also investigated with the AEM-type air electrode, and the overall efficiency was improved due to a remarkable decrease in the potential for the oxygen evolution reaction with Pt–Ir catalysts.

1. Introduction

Electrochemical reactions of oxygen are still challenging issues in electrocatalysis, due to their slow kinetics, despite a long research history [1–3]. Reversible air electrodes that participate in both the reduction and evolution of oxygen are essential for the development of electrically rechargeable metal–air batteries and unitized regenerative fuel cells (URFCs). Electrically rechargeable zinc–air batteries with high energy density have been studied as a potential power source for electric vehicles [4–6]. Recently, rechargeable lithium–air secondary batteries have also been considered and the use of a lithium anode protected by a solid electrolyte and a bi-functional air electrode in aqueous electrolyte has been proposed [7,8]. The problems and trends in the development of reversible air electrodes are described taking those for zinc–air batteries as an example.

Zinc–air primary batteries composed of air electrodes for the cathode and zinc for the anode have already been put into practical application as button cells for use in hearing aids. The theoretical energy density is calculated to be 1312 Wh kg^{-1} of zinc anode [2], which is greater than that of the lithium ion battery, since they can use atmospheric oxygen as a cathode active material. In zinc–air batteries, the reactions described by Eqs. (1) and (2) occur at the anode and the cathode, resulting in the overall reaction in Eq. (3).

$$Zn + 2OH^- \rightarrow ZnO + H_2O + 2e^- \quad (1)$$

$$O_2 + 2H_2O + 4e^- \rightarrow 4OH^- \quad (2)$$

$$Zn + 1/2O_2 \rightarrow ZnO \quad (3)$$

The theoretical voltage of the batteries can be calculated to be 1.65 V based on the potentials of −1.25 V and 0.40 V versus a standard hydrogen electrode, respectively, under standard conditions. The forward and reverse reactions in Eqs. (1)–(3) corresponding to the dissolution and deposition of zinc on the metal electrode and the reduction and evolution of oxygen on the air electrode, take place during the discharging and charging processes of the batteries. Metal–air secondary batteries are promising candidates for next-generation power sources with a high energy density. However, several problems still remain in the development of rechargeable electrodes for both metal and air electrodes.

The development of a reversible air electrode has been challenging for the following reasons. First, the reversibility of the oxygen reduction reaction (ORR) and the oxygen evolution reaction (OER) is poor, since the potentials for the ORR and OER are below and above the theoretical values due to their large overvoltage. This is considered to be a major reason for the reduced energy efficiencies of metal–air secondary batteries. There is an urgent need for the development of bi-functional catalysts that are highly active for both the ORR and OER and are durable under high potential conditions during the OER in the charging process, as an alternative to MnO_2 which is used as a catalyst in zinc–air primary batteries.

* Corresponding author. Tel.: +81 727 51 9653; fax: +81 727 51 9629.
E-mail address: k-yasuda@aist.go.jp (K. Yasuda).

0378-7753/$ – see front matter © 2010 Elsevier B.V. All rights reserved.
doi:10.1016/j.jpowsour.2010.07.074

Several catalysts have been developed for reversible air electrodes, such as perovskite, pyrochlore, and spinel-type metal oxides [2,3]. Perovskite-type $La_{0.6}Ca_{0.4}Co_{0.8}Fe_{0.2}O_3$ is a typical example that has been shown to be stable over 240 cycles during charge–discharge experiments at 100 mA cm^{-2} [9,10]. Other studies have reported that pyrochlore oxides, $Pb_2Ru_2O_{6.5}$ and partial substitutions, enable the ORR with a four-electron process and show excellent reversibility [11,12]. Spinel-type oxides such as $LiMn_{2-x}Co_xO_4$ and $Cu_xCo_{3-x}O_4$ have also been reported to be effective in both the ORR and OER [13–15]. Despite the improved performance of air electrodes, these catalysts do not reach the level required for practical use in secondary batteries.

There are more problems in air electrodes due to their use under highly concentrated alkaline conditions [16,17]. The influence of CO_2 at around 400 ppm in the air on metal–air batteries is unavoidable to some extent, since it is impossible to seal metal–air batteries, which need to take in atmospheric O_2 as an active material. The reaction of alkaline electrolyte with atmospheric CO_2 neutralizes the alkaline electrolyte during long-term operation, which results in a decrease in the ionic conductivity of the electrolyte. Carbonates that precipitate inside the pores of the gas-diffusion electrode by the reaction impede the progress of the ORR and OER on the air electrode. Excessive permeation of the alkaline electrolyte into the air electrode inhibits the diffusion of oxygen to increase the overvoltage of the oxygen reaction on air electrodes and also increases the risk of leakage of alkaline solution for practical use.

A previous study investigated the impact of CO_2 on the charge–discharge behaviors of air electrodes with $La_{0.6}Ca_{0.4}CoO_3$ catalysts in a 15% KOH electrolyte solution by supplying O_2 contaminated by CO_2 [16]. While the potentials for both the ORR and OER are stable for longer than 2500 h with pure O_2, that for the ORR drastically decreased within the first 250 h with O_2 containing 409 and 1000 ppm CO_2. 10,000 ppm CO_2 caused a rapid decrease and increase in the potentials for the ORR and OER within only 10 and 60 h after the start of the experiment, respectively. This rapid increase in the overvoltage was explained by the precipitation of carbonate such as K_2CO_3 on the air electrodes, which has also been considered to be the main factor to explain the degradation of alkaline fuel cells [17]. To overcome these problems, air was supplied to the air electrode after it was passed through a CO_2-filter containing soda lime ($Ca(OH)_2$/NaOH), LiOH, and $Ca(OH)_2$ to reduce the CO_2 concentration.

Several problems related to the negative metal electrode, such as dendrite growth of zinc electrodes while charging remain unsolved, in addition to those for the air electrodes described above [18]. Due to these technical challenges for the electrical recharge of metal–air batteries, previous papers have proposed an alternative charging mode including mechanical charging, in which both the metal used as a negative electrode and the electrolyte solution are changed [19], or an auxiliary third nickel electrode is installed for charging [20].

The present paper proposes a novel solid polymer-type structure of air electrodes. A solid polymer electrolyte was used at the interface between an aqueous alkaline electrolyte and an electrocatalyst of an air electrode layer as a separator and an electrolyte to diminish the problems associated with their use under highly alkaline conditions. The technology related to polymer electrolyte fuel cells (PEFCs) has remarkably progressed and reached a practical level with cation exchange membranes, typically perfluorosulfonate membrane, e.g. Nafion, as polymer electrolyte membranes. Gas-diffusion electrodes that consist of a solid polymer electrolyte and electrocatalysts have achieved improved performance so that they can be operated at a higher current density with smaller Pt content, since a solid polymer electrolyte in the catalyst layer provides three-phase boundaries suitable for the ORR. The use of a solid polymer-type structure is effective for improving the charge–discharge performance of air electrodes at a high current density.

Recently, FCs that use an anion-exchange membrane (AEM) as an alkaline polymer electrolyte membrane have also been developed to decrease the overvoltage or for the use of non-precious metal catalysts [21–24]. In this work, a novel air electrode with an AEM and platinum as the polymer electrolyte membrane and catalyst, respectively, were prepared as a first model to demonstrate this concept, which is represented schematically in comparison with the conventional scheme in Fig. 1. Reduction of the overvoltage was also investigated using AEM-type air electrodes with Pt–Ir catalysts.

2. Concept

The structures of the conventional and AEM-type air electrodes are schematically represented in Fig. 1(a) and (b). In the conventional air electrode composed of a gas-diffusion electrode with permeated alkaline electrolyte solution (KOH) (Fig. 1(a)), atmospheric CO_2 easily dissolves in and reacts with the alkaline electrolyte, which decreases its ionic conductivity and leads to the precipitation of carbonate (K_2CO_3) in the pores of the gas-diffusion electrode. Precipitated carbonate salts in the pores inhibit the diffusion of oxygen, block electrolyte pathways and reduce the effective area for the reaction [1,17,25]. Furthermore, the precipitation of carbonate salts results in expansion and destruction of the electrode structure. In addition, the progressive penetration of the alkaline electrolyte into the electrode may contribute to the inhi-

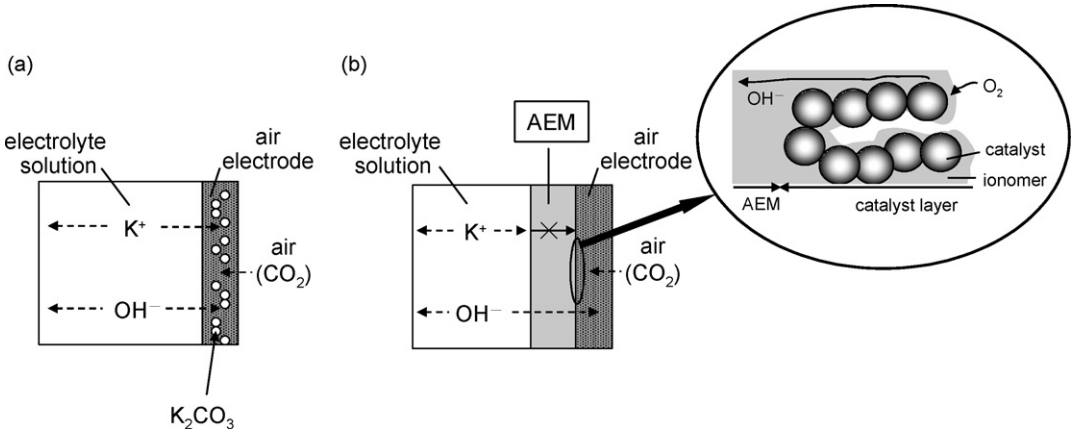

Fig. 1. Schematic illustrations of conventional (a) and AEM-type air electrodes (b).

bition of oxygen diffusion to reduce the performance of the oxygen reaction and bring about electrolyte leakage.

On the other hand, in the AEM-type air electrode, an AEM is placed at the interface between an air electrode layer and the aqueous alkaline electrolyte (Fig. 1(b)). The permeation of cations (K^+) in the alkaline solution into the air electrode is expected to be suppressed by electrostatic repulsion from the cationic functional groups in the AEM, resulting in the inhibition of carbonate precipitation. This inhibition of carbonate precipitation is considered to be one of advantages of AEM-type PEMFCs compared to conventional alkaline fuel cells [26]. An AEM itself can block the incorporation of CO_2 from air to aqueous alkaline electrolyte to some extent. The interfacial structure between the air electrode layer and an AEM is magnified on the right in Fig. 1(b), which shows a structure similar to that of the gas-diffusion electrode in PEFCs. The surface of the catalyst particles is covered with ion-exchange resin (ionomer), and the three-phase boundary between oxygen, catalysts, and ionomer acts as a reaction site. These solid-state structures of AEM-type air electrodes possibly reduce the overpotential and block the permeation or leakage of the alkaline electrolyte into the gas-diffusion layer. In addition, recent developments regarding AEM-type FCs should provide new insights regarding the design of AEM-type air electrodes to enable operation at a high current density comparable to that with PEFCs.

3. Experimental

3.1. Materials

Carbon cloth attached to a hydrophobic fluorocarbon sub-layer on one side with or without Pt black (3 mg cm^{-2}) (purchased from E-TEK) was used as a gas-diffusion electrode or air electrode, respectively. Unsupported Pt and Ir black catalysts (Johnson-Matthey, specific surface area of 27 $m^2\,g^{-1}$ for Pt, >20 $m^2\,g^{-1}$ for Ir) were used as electrocatalysts to prepare air electrodes. An AEM (hydrocarbon-type membrane with quaternary ammonium groups, ion-exchange capacity: 1.4 meq. g^{-1}, thickness: 27 μm) and anion-exchange resin solution (2.0 meq. g^{-1}), both provided by Tokuyama Corporation, were used to prepare polymer electrolyte-type air electrodes. All other chemicals were of analytical grade and used as received.

3.2. Preparation of air electrodes

Air electrode layers were purchased from E-TEK or prepared in-house. In the former case, carbon cloths with Pt black (3 mg cm^{-2}) prepared by E-TEK were used as gas-diffusion electrodes and attached to one side of an AEM by the hot-pressing method. On the other hand, home-made electrode layers were prepared as previously reported for the preparation of electrodes in AEM-type fuel cells [23,24]. Pt and Ir black used as catalysts were suspended in the anion-exchange solution, and the obtained slurry was spread on a PTFE sheet. The catalyst layers (catalysts 3.0 mg cm^{-2}, anion-exchange resin 5 wt.%) were prepared after drying in a vacuum at 80 °C for 1 h. The electrode layers were decal-transferred onto one side of an AEM and further hot-pressed on the hydrophobic-layer side of a carbon cloth supplied as gas-diffusion media.

3.3. Evaluation of air electrode performance

The prepared air electrode with a geometric electrode area of 2 cm^2 was mounted in the cell as shown in Fig. 2. The air electrodes were pushed onto titanium mesh to maintain electrical contact for use as a working electrode (WE). The air electrode was open to the air atmosphere and the opposite side contained 11 ml of KOH electrolyte solution with a reversible hydrogen electrode (RHE) and Pt black electrode fixed in position, which were used as a reference electrode (RE) and a counter electrode (CE), respectively. The dissolved O_2 in the KOH solution was purged by flowing N_2 gas during the evaluation of the air electrode properties. Current–voltage (*I–V*) characteristics for the ORR and OER were obtained galvanostatically using a current pulse generator (Hokuto Denko HC-113) and a digital multimeter at room temperature along with the internal resistance determined by the current-interrupting method. After the initial properties of the ORR and OER were obtained, 100% CO_2 gas was supplied to the air electrode side (right compartment in Fig. 2) for 2 h to accelerate the deterioration of the air electrode. A similar measurement was carried out to obtain *I–V* curves for the ORR and OER, after the air electrode was again exposed to the air atmosphere. Comparison of the results before and after CO_2 flow gave information regarding the effect of CO_2 on the air electrode performance.

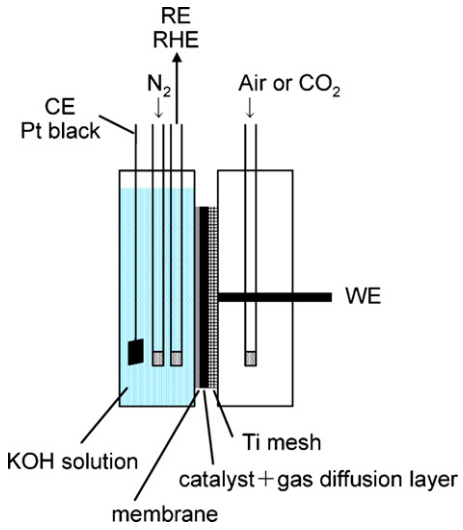

Fig. 2. Cell configuration for evaluating the air electrode properties.

4. Results and discussion

4.1. ORR and OER properties of air electrodes with various KOH concentrations

The ORR and OER properties of air electrodes were evaluated in the alkaline electrolyte with various concentrations of KOH. Fig. 3 shows *I–V* curves for the ORR and OER of the AEM-type air electrodes with a Pt catalyst layer from E-TEK obtained in a KOH aqueous solution, at concentrations of 0.5–8.0 M, and the internal resistance obtained by current-interrupting technique at 5 mA cm^{-2} is shown in parentheses (Ω cm^2). Potentials for the ORR increased with an increase in the KOH concentration up to 6.0 M, whereas those for OER decreased with an increase in the KOH concentration up to 4.0 M. The resistance decreased from 38 to 9 Ω cm^2, and from 38 to 12 Ω cm^2 with an increase in the KOH concentration from 0.5 M to 8.0 M, for the ORR and OER, respectively. The potentials that compensate for the internal resistance obtained in 0.5–8.0 M KOH almost correspond to each other, suggesting that the potential difference is the result of an ohmic drop. A KOH concentration of 4.0 M was sufficient for diminishing the resistance between the WE and the RE to evaluate the performance of air electrodes for both the ORR and OER in this cell configuration. Based on these observations, subsequent experiments were carried out by filling the left compartment of the cell shown in Fig. 2 with 4.0 M KOH aqueous solution.

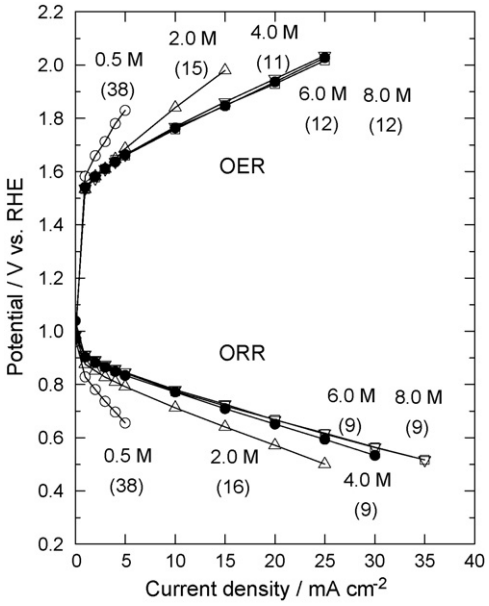

Fig. 3. Potential versus current density curves for the ORR and OER of AEM-type air electrodes with a Pt catalyst in 0.5 M (○), 2.0 M (△), 4.0 M (●), 6.0 M (□), and 8.0 M (▽) KOH electrolyte solution at room temperature, with the resistance at 5 mA cm^{-2} in parentheses (Ω cm^2).

4.2. Effect of CO_2 on the air electrode properties

Comparison of the air electrode properties before and after CO_2 flow gives valuable information about the effect of CO_2 on the air electrode. Fig. 4(a) shows the change in the *I–V* curves for the ORR and OER by the flow of CO_2 for 2 h obtained for the conventional air electrode with a Pt catalyst layer from E-TEK. The potentials changed from ▲ to ●, and showed about a 0.16 V decrease and increase for the ORR and OER at 10 mA cm^{-2}, accompanied by an increase in resistance at 10 mA cm^{-2} from 13 to 27 Ω cm^2 for the ORR and from 14 to 28 Ω cm^2 for the OER. CO_2 lowered and raised the potentials for the ORR and OER, respectively, which corresponds to the remarkable deterioration of air electrode performance by CO_2. The increasing ohmic drop is due to the neutralization of KOH electrolyte solution by CO_2. The potential values that compensated for the internal resistance determined by the current-interrupting method are also shown in Fig. 4(a) by △ and ○ before and after CO_2 was supplied, respectively, which change 0.03 V for the ORR and 0.02 V for the OER. The current densities at the iR compensated potentials of 0.85 V in the ORR and 1.65 V in the OER dropped by about 40% and 24%, respectively after CO_2 was supplied. Therefore, this experiment caused an increase in overvoltage in both the ORR and OER. The same experiments were carried out without a CO_2 supply to consider the reason for the deterioration. The *I–V* curves of the conventional air electrode did not change for either the ORR or OER after 2 h without CO_2 flow. Thus, the increase in overvoltage was not caused by the inhibition of gas diffusion due to the penetration of KOH solution into the gas-diffusion layer, independent of CO_2. Therefore, the increased overvoltages in Fig. 4(a) are considered to correspond to a reduced effective reaction area, probably due to the deposition of carbonate in the gas-diffusion electrode. However, the cause of this reduced effective reaction area is not easy to specify, since we must also consider the effect of increased ionic resistivity of the electrolyte near the three-phase boundary by the dissolution of CO_2. Consequently, the conventional air electrode was severely deteriorated by CO_2 with regard to both internal ohmic resistance and electrode overpotential.

Fig. 4(b) shows the results obtained by similar experiments as in Fig. 4(a) for an AEM-type air electrode with a Pt catalyst layer from

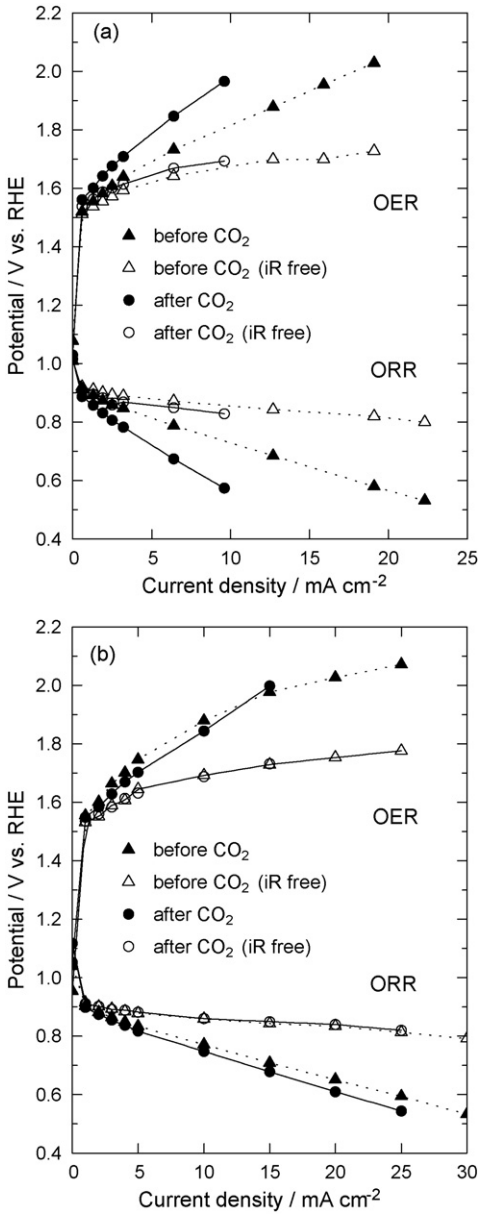

Fig. 4. Potential versus current density curves for the ORR and OER of conventional (a) and AEM-type (b) air electrodes with Pt catalysts before (▲, △) and after (●, ○) CO_2 supply obtained in 4 M KOH at room temperature.

E-TEK. The potential change during CO_2 flow for 2 h is shown as ▲ to ●, which reflects only a 0.02 V decrease in the potentials for the ORR and a decrease of 0.03 V in those for the OER at 10 mA cm^{-2}, with an increase in the resistance from 9 to 12 Ω cm^2 for the ORR and from 11 to 15 Ω cm^2 for the OER. The potential changes for the ORR and OER were quite small compared to those obtained for the conventional air electrode. The potentials that compensated for the internal resistance did not change before and after CO_2 supply, as shown in Fig. 4(b) from △ to ○. This result shows that there appears to be little deterioration after CO_2 supply. AEM used as a separator in the AEM-type air electrode functions to reduce the impact of CO_2 with regard to increasing both the ohmic drop and overvoltage, due to the neutralization of KOH and K_2CO_3 deposition, respectively.

This behavior can be explained as follows. AEM serves to reduce the incorporation of CO_2 into the alkaline electrolyte to prevent the neutralization reaction of KOH with CO_2. Although CO_2 can permeate through the AEM as carbonate ion or gas, the presence of

the AEM delays deterioration. An AEM with anion permselectivity also blocks the permeation of K^+ in the alkaline electrolyte to the air electrode, which presumably suppresses the precipitation of K_2CO_3 in the pores of the air electrode. In addition, the permeation of alkaline electrolyte into the air side (right compartment of the cell shown in Fig. 2) was also lowered by the AEM, suggesting that the AEM also helps to reduce the danger of leakage of highly concentrated alkaline solution.

Other studies have examined zinc-air cells with a polyelectrolyte containing a sulfonium cation group as a separator [27]. It was reported that the polysulfonium prevented the permeation of metal cations (Zn^{2+}) from the anode to the cathode and effectively increased the discharge capacity six fold greater than a commercial separator under alkaline conditions. The AEM-type air electrode proposed in this work is also expected to block the permeation of metal cations besides those from the alkaline electrolyte (K^+), described above. Even though zinc forms anionic complexes such as $[Zn(OH)_4]^{2-}$ in alkaline solution, the AEM may control the penetration of the zinc complex based on the higher permselectivity of OH^- to protect against the deposition of zinc oxide on the air electrode.

Lithium–air batteries that use a lithium metal anode have attracted considerable attention as power sources with a theoretically large energy density of 11,140 Wh kg^{-1}. The deposition of lithium oxide on the air electrode is a serious problem for the development of Li–air batteries. Several studies have elucidated the structure of Li protected by a water-stable lithium-conducting solid electrolyte in combination with an aqueous electrolyte in the vicinity of the air electrode [7,8]. Our proposed structure of the air electrode is applicable to that used in the Li–air batteries with an aqueous electrolyte to inhibit the permeation of Li^+ to the air electrode and oxide deposition.

4.3. Catalysts for reducing overvoltage of the AEM-type air electrode

The low reversibility of the air electrode is known to be a major factor in diminishing the energy efficiency of metal–air batteries, as mentioned above. Catalysts with high activities and low overvoltage toward both the ORR and OER are urgently needed for the development of metal–air secondary batteries. A feasible option to decrease the overvoltage is the use of Pt–Ir catalyst as reported in our previous paper on the development of reversible oxygen electrodes in URFCs using cation exchange membranes [28].

In the present study, mixed Pt black and Ir black in arbitrary ratios were used as catalysts in the AEM-type air electrode prepared in-house to evaluate the ORR and OER properties, as shown in Fig. 4. The results obtained for the AEM-type electrode with various compositions of Pt–Ir catalysts are shown in Fig. 5 with the potentials that compensated for the internal resistance. The potentials for the OER remarkably decreased as much as 0.29 V at 20 mA cm^{-2} upon the addition of 20 wt.% of Ir and also decreased slightly with an increase in the Ir content to 30 and 50 wt.% to diminish the overvoltage for the OER. It has been demonstrated that Ir in Pt–Ir catalysts performs a crucial function in reducing the overvoltage in the OER in alkaline medium, the same as in acid medium [28]. Furthermore, while the ORR characteristics were little influenced by the Ir content, the addition of 20–50 wt.% of Ir slightly increased the potential compared with Pt, unlike the decrease in activity with the addition of Ir in acidic medium [28]. Although platinum is the most active and often-used precious-metal catalyst in the cathode of alkaline FCs, this interesting result shows that Ir is a promising bi-functional catalyst in a reversible air electrode in alkaline media.

The thermodynamic potential of the H_2O/O_2 redox couple is 1.23 V versus RHE. Deviation from this value during the OER or ORR indicates the degree of irreversibility, which deteriorates the efficiency of devices that use an air electrode such as secondary air batteries or URFCs. In this paper, an index of the overall efficiency of an air electrode during discharge (ORR)/charge (OER) cycles was defined as follows. Generally, the terminal voltage values of a device are needed to calculate the energy efficiency. However, the scope of this paper is not limited to a specific negative electrode, and mainly we have considered the single electrode potential of air electrodes. Therefore, to calculate the efficiency, some virtual negative electrode should be assumed as a counter electrode. Thus, a hydrogen electrode is selected for the calculation as a counter electrode on behalf of the negative electrode, i.e.,

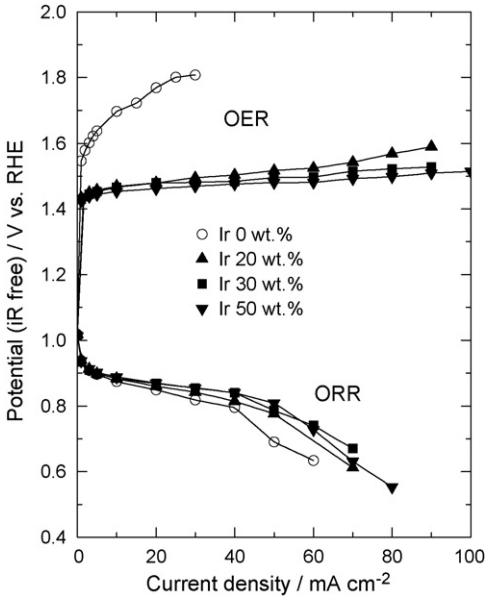

Fig. 5. Potential versus current density curves for the ORR and OER of AEM-type air electrodes with Pt–Ir catalysts of various compositions in 4 M KOH at room temperature.

$$\text{Total efficiency} = (\text{ORR potential vs. RHE}) \div (\text{OER potential vs. RHE}) \times 100\%$$

With this definition, the total efficiency is calculated to be 60%, 51%, 45% at 1, 10, 30 mA cm^{-2}, respectively, for an AEM-type air electrode with a Pt catalyst. The efficiencies improved upon the addition of Ir to Pt catalysts: to 66%, 61%, 58% at 1, 10, 30 mA cm^{-2} for an AEM-type air electrode with a Pt–Ir (Ir: 50 wt.%) catalyst.

The present paper proposed a novel structure for air electrodes using an AEM at the interface of an electrode layer and alkaline electrolyte solution and described the decrease in overvoltage for the ORR and OER, using a Pt-based catalyst. This structure may be effective for improving the performance of aqueous secondary air batteries. This air electrode may also be useful in alkaline-type URFCs. The durability and stability of Pt catalysts at high potential during the OER under charging conditions over the long term have not been experimentally supported. The use of precious-metal catalysts such as Pt may cause problems in terms of their cost and availability for practical use, even though their catalytic activities are relatively excellent. Thus, the development of non-precious metal catalysts for the air electrode in an alkaline electrolyte is desirable for future applications.

5. Conclusions

This work investigated an air electrode that shows excellent activity for both the reduction and evolution of oxygen, as well as good durability during long-term operation in alkaline medium,

which is desired for electrically rechargeable metal–air batteries and alkaline regenerative fuel cells. A polymer electrolyte-type air electrode with an AEM at the interface between the air electrode layer and alkaline electrolyte was proposed to diminish the impact of atmospheric CO_2 on the oxygen reaction properties. The AEM-type air electrode was less influenced by CO_2 even in the accelerated experiment with pure CO_2 compared to conventional air electrodes without an AEM. The AEM blocked the incorporation of CO_2 into the alkaline electrolyte to prevent neutralization of the alkaline electrolyte by CO_2. The AEM with anion permselectivity presumably inhibited the permeation of cations in the alkaline electrolyte to the air electrode to suppress the precipitation of carbonate in the pores of the air electrode. The AEM-type air electrode also successfully reduced the overvoltage for the oxygen evolution reaction with the use of Pt–Ir catalysts.

Acknowledgments

This study was supported by the New Energy and Industrial Technology Development Organization (NEDO) of Japan under the project "Development of High Performance Battery System for Next-Generation Vehicles" (Li-EAD project). The authors are grateful to Tokuyama Corporation for providing membrane samples. The authors also thank Ms. Yumiko Hayashi and Ms. Noriko Maeda for their kind support with the experiments.

References

[1] K. Kinoshita, Electrochemical Oxygen Technology, Wiley, New York, 1992.
[2] L. Jörissen, J. Power Sources 155 (2006) 23–32.
[3] V. Neburchilov, H. Wang, J.J. Martin, W. Qu, J. Power Sources 195 (2010) 1271–1291.
[4] L. Öjefors, L. Carlsson, J. Power Sources 2 (1977/1978) 287–296.
[5] K.F. Blurton, A.F. Sammells, J. Power Sources 4 (1979) 263–279.
[6] J. Goldstein, I. Brown, B. Koretz, J. Power Sources 80 (1999) 171–179.
[7] S.J. Visco, E. Nimon, B. Katz, L.D. Jonghe, M.Y. Chu, 210th ESC Meeting, 2006, Abstract #389.
[8] T. Zhang, N. Imanishi, S. Hasegawa, A. Hirano, J. Xie, Y. Takeda, O. Yamamoto, N. Sammes, J. Electrochem. Soc. 155 (2008) A965–A969.
[9] Y. Shimizu, K. Uemura, H. Matsuda, N. Miura, N. Yamazoe, J. Electrochem. Soc. 137 (1990) 3430–3433.
[10] Y. Shimizu, H. Matsuda, N. Miura, N. Yamazoe, Chem. Lett. 21 (1992) 1033–1036.
[11] J. Prakash, D.A. Tryk, E.B. Yeager, J. Electrochem. Soc. 146 (1999) 4145–4151.
[12] J. Prakash, D.A. Tryk, W. Aldred, E.B. Yeager, J. Appl. Electrochem. 29 (1999) 1463–1469.
[13] N. Li, X. Yan, Y. Jin, S. Li, B. Lin, J. Appl. Electrochem. 29 (1999) 1351–1354.
[14] M. De Koninck, S.-C. Poirier, B. Marsan, J. Electrochem. Soc. 153 (2006) A2103–A2110.
[15] M. De Koninck, S.-C. Poirier, B. Marsan, J. Electrochem. Soc. 154 (2007) A381–A388.
[16] J.-F. Drillet, F. Holzer, T. Kallis, S. Müller, V.M. Schmidt, Phys. Chem. Chem. Phys. 3 (2001) 368–371.
[17] M. Cifrain, K.V. Kordesch, J. Power Sources 127 (2004) 234–242.
[18] C.J. Lan, C.Y. Lee, T.S. Chin, Electrochim. Acta 52 (2007) 5407–5416.
[19] F.R. McLarnon, E.J. Cairns, J. Electrochem. Soc. 138 (1991) 645–664.
[20] T. Sakai, T. Iwaki, Z. Ye, D. Noréus, O. Lindström, J. Electrochem. Soc. 142 (1995) 4040–4045.
[21] K. Matsuoka, Y. Iriyama, T. Abe, M. Matsuoka, Z. Ogumi, J. Power Sources 150 (2005) 27–31.
[22] K. Asazawa, K. Yamada, H. Tanaka, A. Oka, M. Taniguchi, T. Kobayashi, Angew. Chem. Int. Ed. 46 (2007) 8024–8027.
[23] N. Fujiwara, Z. Siroma, S. Yamazaki, T. Ioroi, H. Senoh, K. Yasuda, J. Power Sources 185 (2008) 621–626.
[24] N. Fujiwara, S. Yamazaki, Z. Siroma, T. Ioroi, H. Senoh, K. Yasuda, Electrochem. Commun. 11 (2009) 390–392.
[25] F. Bidault, D.J.L. Brett, P.H. Middleton, N.P. Brandon, J. Power Sources 187 (2009) 39–48.
[26] J.R. Varcoe, R.C.T. Slade, Fuel Cells 5 (2005) 187–200.
[27] E.L. Dewi, K. Oyaizu, H. Nishide, E. Tsuchida, J. Power Sources 115 (2003) 149–152.
[28] T. Ioroi, K. Yasuda, Z. Siroma, N. Fujiwara, Y. Miyazaki, J. Power Sources 112 (2002) 583–587.